Inorganic Chemistry

Communication

pubs.acs.org/IC

Inelastic X-ray Scattering of a Transition-Metal Complex ($FeCl_4^-$): Vibrational Spectroscopy for All Normal Modes

Weibing Dong,[†,§,△] Hongxin Wang,[†,‡,△] Marilyn M. Olmstead,[†] James C. Fettinger,[†] Jay Nix,[‡] Hiroshi Uchiyama,[∥] Satoshi Tsutsui,[∥] Alfred Q. R. Baron,[∥,⊥] Eric Dowty,[¶] and Stephen P. Cramer*[,†,‡]

[†]Department of Chemistry, University of California, Davis, California 95616, United States

[‡]Physical Biosciences Division, Lawrence Berkeley National Laboratory, Berkeley, California 94720, United States

[∥]Research and Utilization Division, SPring-8/JASRI, 1-1-1 Kouto, Sayo, Hyogo 679-5198, Japan

[⊥]Materials Dynamics Laboratory, RIKEN SPring-8 Center, 1-1-1 Kouto, Sayo, Hyogo 679-5148, Japan

[¶]Shape Software, 521 Hidden Valley Road, Kingsport, Tennessee 37663, United States

Supporting Information

ABSTRACT: The tetraethylammonium salt of the transition-metal complex $FeCl_4^-$ has been examined using inelastic X-ray scattering (IXS) with 1.5 meV resolution (12 cm^{-1}) at 21.747 keV. This sample serves as a feasibility test for more elaborate transition-metal complexes. The IXS spectra were compared with previously recorded IR, Raman, and nuclear resonant vibrational spectroscopy (NRVS) spectra, revealing the same normal modes but with less strict selection rules. Calculations with a previously derived Urey-Bradley force field were used to simulate the expected Q and orientation dependence of the IXS intensities. The relative merits of IXS, compared to other photon-based vibrational spectroscopies such as NRVS, Raman, and IR, are discussed.

Vibrational spectroscopy is one of the most fundamental tools for inorganic chemistry. The standard techniques, IR and Raman spectroscopy, are powerful probes of structure and dynamics, and they complement each other with different selection rules.[1] Particle scattering methods, such as inelastic neutron scattering (INS) and high-resolution electron energy loss, also have their merits but have respective requirements for multigram samples or an ultrahigh-vacuum environment. One synchrotron-based technique, nuclear resonant vibrational spectroscopy (NRVS),[2] has shown great potential for the characterization of materials and metalloproteins, but it can only be applied to isotopes such as ^{57}Fe with appropriate excited-state energies and lifetimes. A second synchrotron-based technique, resonant inelastic X-ray scattering (RIXS), at the moment is limited to several hundred reciprocal centimeter resolution.[3] Here we employ a third synchrotron method, inelastic X-ray scattering (IXS).[4] IXS has previously been applied to pure elements such as carbon in diamond or graphite,[5] binary solid-state compounds such as MgB_2, MgO, and SiC,[6] complex superconductors,[4c] liquids as diverse as water or ^3He,[7] and even DNA and proteins[8] but never to a metal coordination complex.

IXS differs fundamentally from IR, Raman, and RIXS in that it depends on an $\mathbf{A}^2$ term in the Hamiltonian for the interaction of radiation with matter, as opposed to the $\mathbf{p}\cdot\mathbf{A}$ terms relevant to the other methods (where $\mathbf{A}$ is the vector potential and $\mathbf{p}$ is the momentum).[9] Whereas X-ray diffraction Bragg peaks derive from coherent elastic scattering of X-rays, IXS derives from the coherent inelastic scattering of X-rays by phonons in a sample. In fact, much of the thermal diffuse scattering (TDS) seen between diffraction peaks is part of the IXS signal, but in a TDS measurement, there is no attempt to energy-resolve that scattering. Thanks to developments in synchrotron radiation sources and X-ray optics, IXS experiments can resolve scattered radiation with an energy resolution of ~1 meV (8 cm^{-1}). As a test of the feasibility and relevance of this technique for inorganic coordination chemistry, we recorded IXS for a crystal of a tetrahedral iron complex: $(NEt_4)(FeCl_4)$. Despite the small cross section and competition with photoabsorption, we were able to record excellent spectra using an established spectrometer.[4c,10] A representative spectrum (acquired in 24 h) is compared with previously recorded NRVS, Raman, and IR data in Figure 1; experimental details are provided in the Supporting Information.

For an isolated transition-metal complex in tetrahedral T_d symmetry, there are four types of normal modes: A_1 and T_2 stretching motions along with T_2 and E and bending modes. The selection-rule advantage of IXS for seeing these modes, compared to other methods, is clearly visible in Figure 1, where all four of the expected bands are clearly visible. This is in sharp contrast to the IR, NRVS, and Raman spectra, which are each most sensitive to only two out of the four main features. For example, the bands at 119 and 137 cm^{-1} can be attributed to the E and T_2 bend modes, respectively.[11] The former is strong in the Raman spectrum, while the latter is more visible in the IR and NRVS spectra, but both bands are strong in IXS. At higher energies, the bands at 330 and 380 cm^{-1} correspond to the totally symmetric A_1 stretching mode and the T_2 asymmetric stretch. As before, the first band is strong in the Raman spectrum, while the second is mostly visible by IR or NRVS, but both modes are distinct in IXS.

A closer look reveals that the $FeCl_4^-$ asymmetric stretching mode near 380 cm^{-1} is split. This is clearest in the Raman spectrum, where bands at 376 and 389 cm^{-1} are resolved. In

Received: February 9, 2013
Published: May 13, 2013

dx.doi.org/10.1021/ic400353j | Inorg. Chem. 2013, 52, 6767−6769

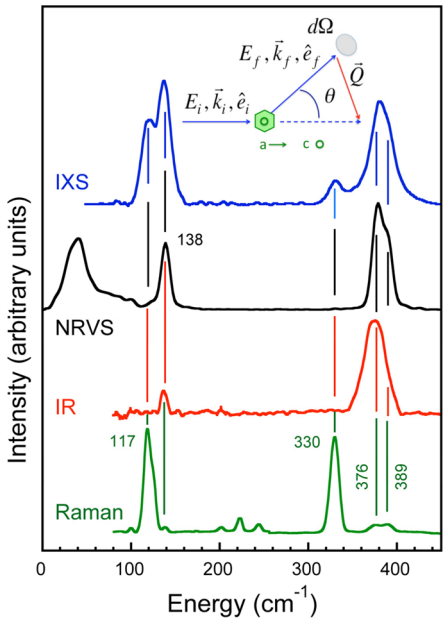

Figure 1. Comparison of IXS for $(NEt_4)(FeCl_4)$ versus other methods. Top to bottom: IXS for crystal with beam along the *a*-axis and *c*-axis perpendicular to the horizontal scattering plane. $\theta = 27°$, ^{57}Fe NRVS,[11] FT-IR, and Raman. Inset: definition of the scattering angle θ and other quantities.

the room temperature crystal structure, the symmetry of the $FeCl_4^-$ ion is better described as C_{3v}, with three shorter Fe−Cl bonds at 2.177 Å and one longer Fe−Cl bond at 2.186 Å. Descent in symmetry from T_d to C_{3v} splits the T_2 modes into E and A_1 modes. This splitting is suggested in IXS because the line width of the A_1 region is 12−14 cm^{-1} (essentially the beamline resolution), while for the T_2 region, it is ∼30 cm^{-1}.

The IXS data in Figure 1 come from just one crystal orientation and scattering angle θ. One strength of this technique is that particular normal modes can be enhanced by the variation of both settings. To illustrate the value of Q- and orientation-dependent IXS for highlighting particular normal modes, we present spectra obtained for different conditions in Figure 2. (At $\chi = 0°$, the crystal *c* axis was vertical and the beam was along the *a* axis. At $\chi = 45°$, the *c* axis was rotated to make a 45° angle with the beam. The additional curves each took 12 h.)

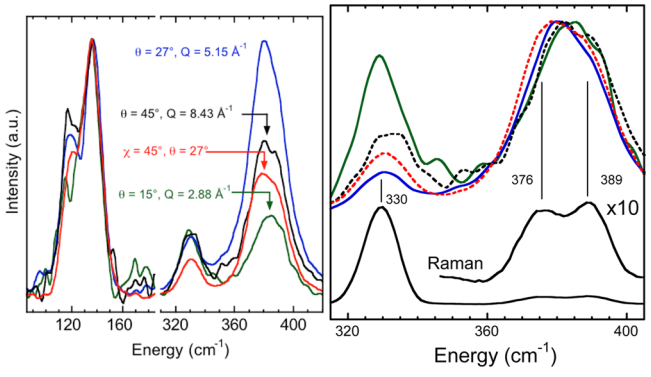

Figure 2. IXS for various Q and crystal orientations. Left: Spectra for χ, θ at (0°, 15°), (0°, 27°), (0°, 45°), and (45°, 27°). Right: stretching-mode-region comparison with the Raman spectrum. (All curves were normalized to the maximum peak height.)

From the data shown in Figure 2, it is clear that there is a strong Q dependence on the relative intensities of the IXS bands. For example, for $\theta = 15°$, the stretching bands are ∼3-fold weaker than the bending modes, while for $\theta = 27°$, the T_2 stretch and T_2 bend are of comparable intensity. There are also wide variations within the stretching region. As is shown better in Figure 2 (right), for $\theta = 15°$, the A_1 stretch intensity is 82% of the T_2 intensity, while for $\theta = 27°$, it is reduced to 24%. Finally, there are also significant variations in the relative intensities for a fixed scattering angle. For example, at $\theta = 27°$, rotation of the crystal by 45° about the *a* axis yields the spectrum with the weakest A_1 band.

With a known crystal structure and force field, all of the observed changes are, in principle, calculable from the well-developed theory behind IXS. This theory has been extensively reviewed elsewhere,[4a,12] so before discussing the representative calculated spectra, we merely summarize the key factors that govern IXS intensities. With initial photon energy E_i and final energy E_f, the phonon energy is given by $E = \hbar\omega \cong E_i - E_f$. As defined in Figure 1, $\vec{k}_i$, $\hat{\varepsilon}_i$, $\vec{k}_f$, and $\hat{\varepsilon}_f$ are the initial and final photon wavevectors and polarizations, respectively, and for scattering angle θ, the momentum transfer is $\hbar\vec{Q} = 2\hbar\,\vec{k}_i \sin(\theta/2)$. The single-phonon cross section for scattering, $\partial^2\sigma/\partial\Omega\,\partial E$, is proportional to $S(\vec{Q},\omega)$, the "dynamical structure factor". Along with terms accounting for phonon population and polarization effects, $S(\vec{Q},\omega)$ is, in turn, proportional to the "inelastic structure factor", $F_{in}(\vec{Q})$, which involves a summation over all of the atoms in the primitive cell and thus for a particular phonon mode:[4,12]

$$F_{in}(\vec{Q}) = \left| \sum_m M_m^{-1/2} f_m(Q)\,[\vec{e}_m^{\,n}(\vec{q})\cdot Q]\,\exp(i\vec{Q}\cdot\vec{r}_m)\,\exp(-w_m) \right|^2$$

In the above expression, atom *m* with mass M_m is located at $\vec{r}_m$ and has X-ray form factor $f_m(Q)$ and Debye-Waller factor $\exp(-w_m)$. The term $\vec{e}_m^{\,n}(\vec{q})$ is the phonon polarization eigenvector for the direction of motion of atom *m* in phonon mode *n* with wavevector $\vec{q}$.[4c] Because, as $Q \to 0$, $f_m(Q) \to Z$, at small angles the strength of the scattering from a particular atom in a sample will vary approximately as Z^2. The overall signal strength depends on the product of three terms: $f_m(Q)$, Q^2, and a polarization factor that goes as $\cos^2\theta$. In practice, this product maximizes at $Q \cong 10$ Å^{-1} for many elements.

The product $\vec{e}_m^{\,n}(\vec{q})\cdot\vec{Q}$, the projection of the phonon polarization onto the total momentum transfer vector $\vec{Q}$, plays a critical role in the observed intensities. Thus, the intensities of the IXS signal can be directly related to the motions of particular atoms in a given normal mode[4a,12] projected onto $\vec{Q}$. Because one can choose different $\vec{Q}$ values by controlling the scattering geometry, IXS can be made more sensitive to particular phonons in a sample. This means that IXS has the flexibility to see *all* of the normal modes for a transition-metal coordination complex. The appearance of the sum inside the magnitude signs means that the intensity is sensitive to the relative phase of the motions within one primitive cell.

The strength of geometry-dependent IXS for highlighting specific normal modes is illustrated in Figure 3. As examples, we show the Q dependence for an incident beam along the crystal *a* axis (with the *c* axis vertical and a horizontal scattering plane) and IXS for different crystal orientations at fixed Q.

dx.doi.org/10.1021/ic400353j | Inorg. Chem. 2013, 52, 6767−6769

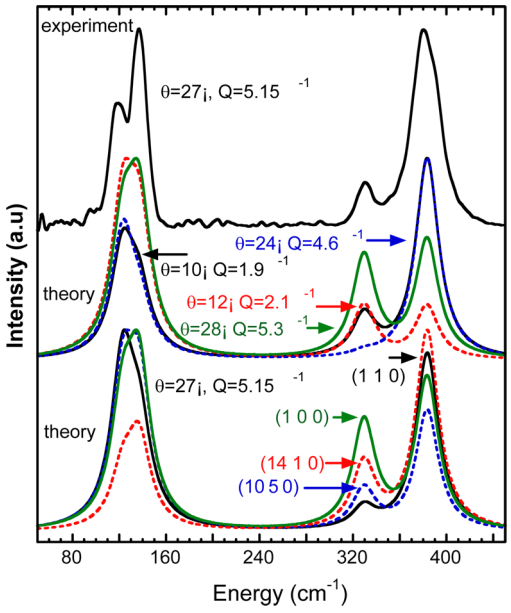

Figure 3. Comparison of the experiment and theory for IXS. Top: data for $\chi = 0°$ and $\theta = 27°$. Middle: calculated IXS for $\chi = 0°$ and different momentum transfers $\theta = 10°$, 12°, 24°, and 28°. Bottom: IXS at $\theta = 27°$ for beams along crystal orientations (1 1 0), (14 1 0), (10 5 0), and (1 0 0).

One striking result from these simulations is the extreme variability in the intensity of the totally symmetric A_1 stretching mode at 330 cm^{-1}. Within the range of θ from 24 to 28°, the strength of this mode varies from almost as strong as the T_2 mode to nearly invisible. A similar variability in the relative intensities is observed for different crystal orientations at a fixed scattering angle. From a practical point of view, this ability to enhance or diminish particular normal modes should assist the detailed assignment of vibrational features in complex spectra.

In summary, the current results show that high-quality IXS spectra can be obtained for a transition-metal complex in a few hours at a third-generation synchrotron radiation source. IXS intensities are amenable to straightforward calculation from a given structure and force field, with none of the complexities involved in the calculation of IR or Raman spectra. Compared to NRVS, IXS has the advantage of applicability to any element in the periodic table, and compared to INS, IXS requires orders of magnitude less material. The Q dependence allows one to enhance the visibility of particular normal modes. There is also a benefit from the orientation dependence of single-crystal spectra, but it has been shown by others that powder spectra are also informative.[12b] Although it has the limitations of a bulk-sensitive technique, there should be many applications in coordination chemistry where selection rules or other constraints preclude the use of more conventional vibrational methods and where IXS will shine as a technique that allows any desired normal mode to be observed.

■ ASSOCIATED CONTENT

Supporting Information

Experimental details for sample preparation and crystallographic results concerning phase transformations at different temperatures. This material is available free of charge via the Internet at http://pubs.acs.org.

■ AUTHOR INFORMATION

Corresponding Author

*E-mail: spjcramer@ucdavis.edu.

Present Address

§W.D.: Department of Biochemistry, The Pennsylvania State University, University Park, PA 16802.

Author Contributions

△These authors have equal contribution to this work.

Notes

The authors declare no competing financial interest.

■ ACKNOWLEDGMENTS

This work was funded by NIH Grant GM-65440 (to S.P.C.) and the DOE Office of Biological and Environmental Research (S.P.C.). The experiments were performed at BL35XU of SPring-8 with the approval JASRI (Proposal No. 2011B1361).

■ REFERENCES

(1) Nakamoto, K. *Infrared & Raman Spectra of Inorganic & Coordination Compounds*, 5th ed.; Wiley-Interscience: New York, 1997.

(2) Seto, M.; Yoda, Y.; Kikuta, S.; Zhang, X. W.; Ando, M. *Phys. Rev. Lett.* **1995**, *74*, 3828−3831.

(3) van Schooneveld, M. M.; Gosselink, R. W.; Eggenhuisen, T. M.; Al Samarai, M.; Monney, C.; Zhou, K. J.; Schmitt, T.; de Groot, F. M. F. *Angew. Chem.* **2013**, *1170*, 3828−3831.

(4) (a) Burkel, E. *J. Phys.: Condens. Matter* **2001**, *13*, 7627−7644. (b) Krisch, M.; Sette, F. *Light Scattering in Solids IX*; Springer-Verlag: Berlin, 2007; Vol. *108*, pp 317−369. (c) Baron, A. Q. R. *J. Spect. Soc. Jpn.* **2009**, *58*, 205−214 (Japanese) arXiv 0910.5764 (English).

(5) (a) Kulda, J.; Kainzmaier, H.; Strauch, D.; Dorner, B.; Lorenzen, M.; Krisch, M. *Phys. Rev. B* **2002**, *66*, 241202. (b) Maultzsch, J.; Reich, S.; Thomsen, C.; Requardt, H.; Ordejón, P. *Phys. Rev. Lett.* **2004**, *92*, 075501.

(6) (a) Baron, A. Q. R.; Uchiyama, H.; Tanaka, Y.; Tsutsui, S.; Ishikawa, D.; Lee, S.; Heid, R.; Bohnen, K. P.; Tajima, S.; Ishikawa, T. *Phys. Rev. Lett.* **2004**, *92*, 197004. (b) Fukui, H.; Katsura, T.; Kuribayashi, T.; Matsuzaki, T.; Yoneda, A.; Ito, E.; Kudoh, Y.; Tsutsui, S.; Baron, A. Q. R. *J. Synchrotron Rad.* **2008**, *15*, 618−623. (c) Strauch, D.; Dorner, B.; Ivanov, A.; Krisch, M.; Serrano, J.; Bosak, A.; Choyke, W. J.; Stojetz, B.; Malorny, M. *Mater. Sci. Forum* **2006**, *527−529*, 689−694.

(7) (a) Sette, F.; Ruocco, G.; Krisch, M.; Bergmann, U. *Phys. Rev. Lett.* **1995**, *75*, 850−853. (b) Seyfert, C.; Simmons, R. O.; Sinn, H.; Arms, D. A.; Burkel, E. *J. Phys.: Condens. Matter* **1999**, *11*, 3501.

(8) (a) Liu, Y.; Chen, S. H.; Berti, D.; Baglioni, P.; Alatas, A.; Sinn, H.; Alp, E.; Said, A. *J. Chem. Phys.* **2005**, *123*, 2235−2245. (b) Liu, D.; Chu, X. Q.; Lagi, M.; Zhang, Y.; Fratini, E.; Baglioni, P.; Alatas, A.; Said, A.; Alp, E.; Chen, S. H. *Phys. Rev. Lett.* **2008**, *101*, 135501.

(9) Baron, A. Q. R.; Uchiyama, H.; Tsutsui, S.; Tanaka, Y.; Ishikawa, D.; Sutter, J. P.; Lee, S.; Tajima, S.; Heid, R.; Bohnen, K.-P. *Physica C* **2007**, *456*, 83−91.

(10) Baron, A. Q. R.; Tanaka, Y.; Goto, S.; Takeshita, K.; Matsushita, T.; Ishikawa, T. *J. Phys. Chem. Solids* **2000**, *61*, 461−465.

(11) Smith, M. C.; Xiao, Y.; Wang, H.; George, S. J.; Coucovanis, D.; Koutmos, M.; Sturhahn, W.; Alp, E. E.; Zhao, J.; Cramer, S. P. *Inorg. Chem.* **2005**, *44*, 5562−5570.

(12) (a) Burkel, E. *Rep. Prog. Phys.* **2000**, *63*, 171−232. (b) Sinha, S. K. *J. Phys.: Condens. Matter* **2001**, *13*, 7511−7523. Fischer, I.; Bosak, A.; Krisch, M. *Phys. Rev. B* **2009**, *79*, 134302.